Intra-procedural dual phase cone beam computed tomography has a better diagnostic accuracy over pre-procedural MRI and MDCT in detection and characterization of HCC in cirrhotic patients undergoing TACE procedure

Pierleone Lucatelli, Gianluca De Rubeis, Luca Ginnani Corradini, Fabrizio Basilico, Michele Di Martino, Quirino Lai, Stefano Ginanni Corradini, Alessandro Cannavale, Pier Giorgio Nardis, Mario Corona, Luca Saba, Carlo Catalano, Mario Bezzi

PII: S0720-048X(19)30456-5

DOI: https://doi.org/10.1016/j.ejrad.2019.108806

Reference: EURR 108806

To appear in: *European Journal of Radiology*

Received Date: 18 September 2019

Revised Date: 28 November 2019

Accepted Date: 19 December 2019

Please cite this article as: Lucatelli P, De Rubeis G, Ginnani Corradini L, Basilico F, Di Martino M, Lai Q, Ginanni Corradini S, Cannavale A, Nardis PG, Corona M, Saba L, Catalano C, Bezzi M, Intra-procedural dual phase cone beam computed tomography has a better diagnostic accuracy over pre-procedural MRI and MDCT in detection and characterization of HCC in cirrhotic patients undergoing TACE procedure, *European Journal of Radiology* (2019), doi: https://doi.org/10.1016/j.ejrad.2019.108806

Intra-procedural dual phase cone beam computed tomography has a better diagnostic accuracy over pre-procedural MRI and MDCT in detection and characterization of HCC in cirrhotic patients undergoing TACE procedure

Authors:

Pierleone Lucatelli MD, PhD EBIR (Corresponding Author)

Vascular and Interventional Radiology Unit, Department of Diagnostic of Radiological, Oncological and Anatomopathological Sciences. Sapienza University of Rome,

Viale del Policlinico, 155, 00161 Rome RM, Italy

pierleone.lucatelli@gmail.com

Gianluca De Rubeis MD

Vascular and Interventional Radiology Unit, Department of Diagnostic of Radiological, Oncological and Anatomopathological Sciences. Sapienza University of Rome,

Viale del Policlinico, 155, 00161 Rome RM, Italy

derubeis.gianluca@gmail.com

Luca Ginnani Corradini MD

Vascular and Interventional Radiology Unit, Department of Diagnostic of Radiological, Oncological and Anatomopathological Sciences. Sapienza University of Rome,

Viale del Policlinico, 155, 00161 Rome RM, Italy

lucaginannicorradini@gmail.com

Fabrizio Basilico MD

Vascular and Interventional Radiology Unit, Department of Diagnostic of Radiological, Oncological and Anatomopathological Sciences. Sapienza University of Rome,

Viale del Policlinico, 155, 00161 Rome RM, Italy

fabribasi@gmail.com

Michele Di Martino MD

Vascular and Interventional Radiology Unit, Department of Diagnostic of Radiological, Oncological and Anatomopathological Sciences. Sapienza University of Rome,

Viale del Policlinico, 155, 00161 Rome RM, Italy

micdimartino@hotmail.it

Quirino Lai MD, PhD

Department of General Surgery and Organ Transplantation, Sapienza University of Rome,

Viale del Policlinico, 155, 00161 Rome RM, Italy

Quirino.lai@uniroma1.it

Stefano Ginanni Corradini MD, Prof

Department of Translational and Precision Medicine, Sapienza University of Rome,

Viale del Policlinico, 155, 00161 Rome RM, Italy

Stefano.corradini@uniroma1.it

Alessandro Cannavale MD

Vascular and Interventional Radiology Unit, Department of Diagnostic of Radiological, Oncological and Anatomopathological Sciences. Sapienza University of Rome,

Viale del Policlinico, 155, 00161 Rome RM, Italy

alessandro.cannavale@hotmail.com

Pier Giorgio Nardis MD

Vascular and Interventional Radiology Unit, Department of Diagnostic of Radiological, Oncological and Anatomopathological Sciences. Sapienza University of Rome,

Viale del Policlinico, 155, 00161 Rome RM, Italy

p.nardis@gmail.com

Mario Corona MD

Vascular and Interventional Radiology Unit, Department of Diagnostic of Radiological, Oncological and Anatomopathological Sciences. Sapienza University of Rome,

Viale del Policlinico, 155, 00161 Rome RM, Italy

mario.corona@uniroma1.it

Luca Saba MD, Prof

Department of Medical Imaging, Azienda Ospedaliero Universitaria (A.O.U.) of Cagliari-Polo di Monserrato, Via Ospedale, 54, 09124 Cagliari CA, Italy

lucasabamd@gmail.com

Carlo Catalano MD, Prof

Vascular and Interventional Radiology Unit, Department of Diagnostic of Radiological, Oncological and Anatomopathological Sciences. Sapienza University of Rome,

Viale del Policlinico, 155, 00161 Rome RM, Italy

Carlo.catalano@uniroma1.it

Mario Bezzi MD, Prof, EBIR

Vascular and Interventional Radiology Unit, Department of Diagnostic of Radiological, Oncological and Anatomopathological Sciences. Sapienza University of Rome,

Viale del Policlinico, 155, 00161 Rome RM, Italy

Mario.bezzi@uniroma1.it

Corresponding Author:

Pierleone Lucatelli MD, PhD, EBIR

"Sapienza" University of Rome,

Vascular and Interventional Radiology Unit, Department of Diagnostic Service. Sapienza University of Rome, Italy

Viale Regina Elena 324,

00161, Rome, Italy.

Telephone: +39 06 44 68 587

Fax: +39 06 49 02 43

e-mail: pierleone.lucatelli@gmail.com

Highlights

- Accuracy and NPV of DP-CBCT were higher than MDCT and MRI (94%vs78%; 92%vs30%, respectively)
- Confirmed HCC visible only in DP-CBCT were 54/243 (22%)
- Nodules' diameter was higher in DP-CBCT than MDCT and MRI (mean increase 1.6 mm; + 7.5%, p< 0.05)

Abstract

Purpose

This study was directed to compare diagnostic accuracy of dual-phase cone beam computed tomography (DP-CBCT) vs pre-procedural second line imaging modality (SLIM [multidetector computed tomography and magnetic resonance imaging]) to detect and characterize hepatocellular carcinoma (HCC) in cirrhotic patients with indication for trans-arterial chemoembolization (TACE).

Methods

This is a single centre, retrospective, and observational study. Exclusion criteria were not-assisted DP-CBCT TACE, and unavailable follow-up SLIM. We evaluated 280 consecutive patients (January/2015-Febraury/2019). Seventy-two patients were eligible. Three radiologists in consensus reviewed: pre-procedural SLIM, DP-CBCT, and SLIM at follow-up, with 4 months of interval between each reading. Hyper-vascular foci (HVF) were detected and characterized. Diameter was recorded. Radiological behaviour, according to LI-RADS criteria, of HFV throughout follow-up time was the reference standard. Diagnostic accuracy was calculated for pre-procedural SLIM and DP-CBCT and evaluated through receiver operating

characteristic curve. HVF only visible on DP-CBCT (defined as occult) were analysed. Tumour diameters were compared.

Results

Median time between pre-procedural SLIM and DP-CBCT and between DP-CBCT and definitive radiological diagnosis of HVF were 46.0 days (95%CI 36.5-55.0) and 30.5 days (95%CI 29.0-33.0), respectively.

DP-CBCT had a better diagnostic performance than pre-examination SLIM (sensitivity 99%vs78%; specificity 89%vs85%; PPV 99%vs99%; NPV 92%vs30%; and accuracy 94%vs79%). DP-CBCT diagnosed 63 occult HVF. Occult HCC were 54/243 (22.2%). Six were occult angiomas. Three were false positive. Mean diameter was significantly higher in DP-CBCT vs pre-procedural SLIM (+7.5% [95%CI 3.7-11.3], $p<0.05$).

Conclusions

DP-CBCT has a better diagnostic accuracy and NPV than pre-procedural SLIM in cirrhotic patients with indication for TACE.

Highlights

- Accuracy and NPV of DP-CBCT were higher than MDCT and MRI (94%vs78%; 92%vs30%, respectively)
- Confirmed HCC visible only on DP-CBCT were 54/243 (22%)
- Nodule'sdiameter was higher in DP-CBCT than MDCT and MRI (mean increase 1.6 mm; + 7.5%, $p < 0.05$)

Key words

- Hepatocellular Cancer
- Therapeutic Chemoembolization
- Cone-Beam Computed Tomography
- Computerized Tomography, X Ray
- Magnetic resonance imaging

Abbreviations

BCLC: Barcelona Clinic Liver Cancer trans-arterial chemoembolization

CI: confidence intervals

DP-CBCT: dual phase cone beam computed tomography

HCC: hepatocellular carcinoma

HVF: hyper-vascular foci

MDCT: multidetector computed tomography

MRI: magnetic resonance imaging

ROC: received operator characteristic

RS: reference standard

SLIM: second-line imaging modalities

TACE: trans-arterial chemoembolization

US: ultra-sound

Main Body

Introduction

Hepatocellular carcinoma (HCC) is the fifth most common cancer in the world, accounting for 7% of all cancer-related deaths and showing an increasing trend in the future[1]. In cirrhotic patients, 6-month abdominal ultrasound (US) (sensitivity 58-89%; specificity > 90%) represents the recommended surveillance method, while second-line imaging modalities (multi-detector computed tomography [MDCT] and magnetic resonance imaging [MRI]) are only reserved for better lesion's characterization [2, 3]. In cirrhotic patients with HCC, the imaging interval should be reduced to 3-4 months [3]. Chou et al. highlighted a sensitivity of 84% (95% confidence intervals [CI]=59-95) and a specificity of 99% (95%CI=86-99) for MDCT in a per-patient surveillance setting [4]. In a meta-analysis published by Lee YJ et al., the diagnostic accuracy was higher for MRI than MDCT (80% vs 68%, p< 0.01) [5]. The sensitivity and specificity of MRI rose to 87% and 94% using hepatobiliary phase. [6]. However, the per-lesion sensitivity for sub-centimeter HCC was insufficient in both for MDCT and MRI (64% vs 77%; 73% vs 81%; p<0.05, respectively) [5].

According to the Barcelona Clinic Liver Cancer (BCLC) classification [7], trans-arterial chemoembolization (TACE) is indicated for intermediate stage disease. Both Cardiovascular and Interventional Radiological Society of Europe[8] and Society of Interventional Radiology [9] quality improvement guidelines emphasized the role of cone-beam computed tomography (CBCT) in assisting TACE procedures. CBCT is an acquisition obtained by a rotation of an angiographic suite equipped with flat panel detector without patient repositioning [10]. Furthermore, CBCT can be performed before TACE procedure and using contrast media injection as multiphasic imaging. In particular, CBCT has gained attention as a helper tool for tumor detection, intraprocedural guidance and treatment assessment during TACE [10-12]. More specifically, dual-phase (DP) CBCT showed a sensitivity of 93.9% for HCC detection, when compared with MRI [13] and with CBCT early-arterial or delayed arterial phase (72 %; 87 %, respectively) [14]. Moreover, authors report the ability of monophasic CBCT to depict more hyper-vascular foci (HVF) defined as occult nodules in respect to pre-procedural second-line imaging modalities (SLIM), (rate: 11.5-28.7%) [15, 16]. The rationale to compare the diagnostic performance of DP-CBCT vs SLIM is based on several hypotheses. Firstly, CBCT has higher contrast-to-noise ratio and spatial resolution respect to MDCT [15, 17]. Secondly, intra-arterial injection of contrast media in CBCT enhances the contrast-to-noise ratio of the HVF[18]. Third, a nodule with typical radiological behavior on multiphasic CBCT can be highly consistent with HCC. Thus, the potential advantage of delayed second-phase acquisitions relies on the possibility of intra-procedurally assessing the nature of HVF.

The objective of this study is to evaluate and compare the diagnostic performance (sensitivity, specificity, positive and negative predictive value and accuracy) of DP-CBCT vs. pre-procedural SLIM, using

as reference standard (RS) the behavior of the hyper-vascular foci (HVF)[HCC and angioma] at SLIM follow-up in cirrhotic patients undergoing TACE for HCC.

Material and Methods

This study was approved by the ethical institutional review board. Informed consent for the procedure as for anonymized publication was obtained from all the individual participants included in this study.

The manuscript was drafted according to Standards for Reporting Diagnostic accuracy studies (STARD) guideline.[19]

This is a cohort, retrospective single center study. We retrospectively reviewed all patients that underwent TACE since January 2015 (installation of CBCT software) to February 2019. The indication for TACE was given in all cases by a multidisciplinary board formed by a transplant surgeon, an interventional radiologist, a body radiologist, and a hepatologist. We included in the study all patients treated with DP-CBCT-assisted TACE. Exclusion criteria were a) TACE not assisted by DP-CBCT; and, b) no SLIM at follow-up (**Figure 1**).

Second-line imaging modality (MDCT or MRI) protocol

MDCT

MDCT was performed using a 1st Generation Dual Source CT scanner (SOMATOM DEFINITION; Siemens, Erlangen, Germany). The phases included in the protocol were: unenhanced, late arterial, venous and delayed. Late arterial-phase delay was defined using bolus tracking with automated scan triggering (CARE Bolus CT; Siemens, Erlangen, Germany) with a delay of 18 s after trigger threshold of 150 HU in supra-coeliac abdominal aorta. All patients received 1.7 mL/kg body weight of iomeprol (Iomeron 370; Bracco, Milan, Italy)[20]. Contrast media was administrated via a dual chamber mechanical power injector (Stellant D CT; Medrad, Indianola, Pennsylvania) at a rate of 4.5 mL/s in a antecubital vein (18 Gauge needle). The contrast bolus was followed by a flush of 40 ml saline at the same injection rate. The tube scan parameters were modulated using CARE Dose (Siemens, Erlangen, Germany) and CARE kV (Siemens, Erlangen, Germany) : voltage reference, 120 kVp; current reference, 210 mA; gantry rotation time, 0.33 seconds; pitch, 1; slice thickness, 3 mm[15].

MRI

MRI was performed at 3 T MR scanners (Discovery MR750. GE HealthCare, Milwaukee, WI, USA) with an 8-channel phased array coils. Protocols included T2-weighted single-shot sequence, a T2-weighted fast spin-echo sequence with fat saturation, and a transverse breath-hold 3D T1- weighted fat-suppressed spoiled gradient-recalled echo sequence before and after dynamic injection of contrast medium. A free-breathing, fat-suppressed, single-shot echoplanar diffusion-weighted MR sequence was obtained before contrast injection with b values of 0, 50, 400 and 800 s/mm^2. A total of 0.05 mmol/kg of body weight (0.1 ml/kg) of

Gd-BOPTA or 0.025 mmol/kg of body weight (0.1 ml/ kg) of Gd-EOB-DTPA were administrated followed by 15-ml saline solution flush were administered at 2 ml/s with a power injector. Post contrast images were acquired during the late hepatic arterial, hepatic venous, and late dynamic phases, respectively, as well as during the hepatobiliary phase. Timing for the initial post-contrast arterial phase acquisition was determined using an automated bolus detection technique (SmartPrep, General Electric). Hepatobiliary phase was acquired at 20 min (Gd-EOB-DTPA) or at 75 minutes (Gd-BOPTA) after injection[21].

CBCT

All the procedures were performed by the same interventional radiologist (BLIND, > 10 years of experience) in a dedicated angiography suite equipped with a ceiling-mounted angiographic C-arm system and a 30*40-cm flat-panel detector (Artis Zee; Siemens, Erlangen, Germany). Digital subtracted angiography and CBCT were acquired using a power injector (Mark V ProVis; Medrad, Indianola, Pennsylvania) after the 4-F catheter had been positioned within the proper hepatic artery. CBCT protocol included: arterial and delayed phases. All intraprocedural cone-beam CT acquisitions were performed with the same contrast medium (Iomeron 370; Bracco, Milan, Italy) diluted at a 1:3 ratio with sterile saline solution to avoid streak artefacts. Power injector parameters were set to 4 mL/s and intraarterial injection lasted 15 seconds to maintain arterial tree enhancement during CBCT acquisition; first CBCT acquisition started after 8 seconds of injection, second delayed phase CBCT was acquired after 35 seconds from the beginning of the injection. The C-arm rotates 200° around the patient in 5 seconds, acquiring images every 0.8° at 60 frames per second for a total of 248 images; the estimated detector dose was 0.36 µGy per frame. Reconstruction images lead to a 512*512*387 matrix and isotropic resolution of 0.49 mm, resulting in a 25*25*19-cm field of view. The liver was positioned symmetrically in the isocenter of the C-arm rotation[15].

Follow-up

Scheduled second-line imaging modality (MDCT or MRI) followed the protocol of our Institution developed by multidisciplinary board, based on the European Association for the Study of the Liver (EASL) and the European Organization for Research and Treatment of Cancer (EORTC). In particular, the first imaging was performed at least after 1 month following TACE procedure, thereafter every three months [1, 22]. The proportion of patients experienced MRI or MDCT as pre-procedural or follow-up imaging reproduced the retrospective nature of the study by reflecting the real-life of a high-volume tertiary referral liver transplantation center. This distribution was due to machines availability, patients' contraindications and patients' preferences.

Imaging evaluation

Three different expert body radiologists (>7 years of experience) evaluated each dataset of imaging technique (pre-TACE second-line imaging modalities, intra-procedural DP-CBCT, or all the available SLIM

follow-up imaging), with 4 months between each modality assessment. In case of disagreement a consensus was found.

The radiological diagnosis of HCCs was performed at MDCT/MRI according to typical radiological behavior of HVF in cirrhotic liver following LI-RADS criteria [23-26]. LI-RADS criteria[26] were adapted to DP-CBCT imaging, although these criteria were not specifically addressed for this radiological technique.

Reference Standard (RS) was defined as the evolution of focal liver lesion throughout all available follow-up time until the evidence of typical radiological HCC appearance. All HVF and their diameter were recorded. If the radiological behavior of an HVF was still equivocal at the last follow-up SLIM, the nodule was considered as non-HCC.

Study outcome measurements

The primary outcome was the diagnostic performance for detection and characterization of HVF within the liver, in patients with HCC and an indication for TACE, for both pre-procedural SLIM and intra-procedural DP-CBCT.

The secondary outcome was the analysis of occult HVF defined as a nodule visible at the intra-procedural DP-CBCT, confirmed by the RS, and not visible at the pre-procedural SLIM.

The tertiary outcome was the diameter dimension comparison between pre-procedural SLIM, intra-procedural DP-CBCT and RS. The diameter was measured in venous phase for SLIM and delayed phase for DP-CBCT

Statistical analysis

Dichotomous variables were reported as numbers and percentages. The Kolmogorov-Smirnov Z test was performed to assess normality distribution for all variables tested. Continuous normal variables were expressed as mean ± standard deviation. Continuous non-normal variables were expressed as median and 95%CI. The Wilcoxon's test and the Bland and Altman plot were used to compare the tumor diameter as paired between pre-procedural SLIM and intra-procedural DP-CBCT. The behavior of focal liver lesion in all the available follow-up second-line imaging modalities was considered the RS. The diagnostic performance of the pre-TACE second-line imaging modality and DP-CBCT were compared with the RS. Sensitivity, specificity, predictive positive value (PPV), predictive negative value (NPV) and accuracy were evaluated through a Receiver Operating Characteristic (ROC).

The sample size was calculated using an expected area under the curve for DP-CBCT of 0.947 and for pre-exam SLIM of 0.771 as previous published [27]. Alpha- and beta-errors were set at 0.01. According to these parameters, the calculated predicted sample size was of 161 HVF. Considering a 15% of cases expected to

be lost at follow-up, the minimum sample size required for the study was therefore set at 185 HVF. P values < 0.05 were considered statistically significant.

Statistical analysis was performed, and the graph was plotted using MedCalc 8.0 software (MedCalc, Mariakerke, Belgium).

Results

We retrospectively reviewed 280 consecutive patients undergoing TACE from January 2015 to February 2019. Two hundred and two patients were excluded from the final analysis because they were not treated with a DP-CBCT-assisted TACE. Of the remaining 78 patients treated with 97 DP-CBCT-assisted TACE procedures, four (five TACE) were further excluded because of non-availability of SLIM at follow-up. Among these latter patients, two were censored for liver transplantation. Lastly, 72 cases were enrolled for the final analysis. Of these, 11 patients performed more than one TACE (nine patients = two TACE; one patient= three TACE; one patient = six TACE for a total of 18 re-TACE) (see the detailed **Figure 1**).

The demographic and TACE detailed information were given in **Table 1.**

The median time between pre-examination SLIM and TACE was 46.0 days (95%CI 36.5-55.0). The median follow-up time to the definitive radiological diagnosis of occult foci was 30.5 days (95%CI 29.0-33.0) (see **Figure 2.** for time frame distribution). The median follow-up time was 9 months (95% CI 7.0-10.1).

Diagnostic performance

In the 72 patients enrolled in this study, pre-procedural SLIM detected 209 HVF. Of these, 193/209 (92.3%) were diagnosed as HCCs. In 33/193 (17.1%) lesions, the diagnosis was done using MRI. Among the detected lesions, 161/193 (83.4%) presented a diameter > 10 mm (median diameter 16.0 mm [95%CI 14.0-18.2, min 6.0 mm, max 88.0 mm]).

The intra-procedural DP-CBCT diagnosed 259 HVF, with 244 of them (94.2%) diagnosed as HCCs. Hundred-ninety-two/244 (78.7%) lesions, had a diameter > 10 mm. The median diameter of the HCC at intra-procedural CBCT was 15.0 mm (95%CI 13.8 to 17.0, min 6.0 mm, max 82.0 mm).

Finally, 261 HVF were diagnosed at RS: among them, 243 (93.1%) were HCC, while the remaining 18 were hemangiomas.

Compared with RS, the intra-procedural DP-CBCT had a better diagnostic performance than pre-examination SLIM (sensitivity 99% vs 78%; specificity 89% vs 85%; PPN 98% vs 99%; NPV 92% vs 30%; and accuracy 94% vs 82%) (**Table 1** and **Figure 5** showed the detailed analysis).

Intra-procedural DP-CBCT was able to diagnose 63 occult HVF. Among these, 57/63 (90.0%) presented a typical radiological behavior for HCC and, therefore, they were categorized as HCC. However, three of 57

(5.3%) lesions were identified as false positives due to the absence of significant wash-out at RS until the last available imaging (29, 28 and 28 days, respectively). The maximum diameter of these lesions was 23 mm, 8 mm and 7 mm, respectively. Therefore, according to RS, the true positive occult HCC were 54/243 (22.2%). The median diameter of occult HCC was 10.0 mm (95%CI 9.0-11.0). In particular, 33/54 (61%) occult nodules had a maximum diameter >10 mm, with 16/33 (48.5%) being placed in another hepatic segment in respect to the target lesion, and 3/16 (18.9%) in the contralateral hepatic lobe (For more details, see **Flowchart 2,Figure 3 and Figure 4).** Among patients with occult HCCs, 32/38 (84%) were multi-nodular and 6/38 (16%) were uni-nodular at pre-procedural SLIM; the indications for TACE were: palliative 16/38 (42%), bridging for liver transplantation 13/38 (34%), debulking for liver resection 3/38 (8%), and downstaging 6/38 (16%).

The intra-procedural DP-CBCT diameter (mean 19.0 mm; 95%CI 16.3-21.0) was significantly larger as compared to the pre-procedural SLIM (mean 16.0 mm; 95%CI 15.0-19.7). The Bland-Altman plot (**Figure 6**) showed a significant systematic increase of the lesion diameter between intra-procedural CBCT and pre-procedural SLIM (mean increase 1.6 mm; 95%CI 0.8-2.4) Reporting this datum in percentage, a mean 7.5%-increase of the lesions was reported ([95%CI 3.7-11.3; $p< 0.05$).

Discussion

The main result of this study is that intra-procedural DP-CBCT has a better diagnostic performance if compared with pre-procedural SLIM in HVF detection and characterization (accuracy 98% vs 79%).

The worldwide-accepted reference standard imaging for diagnosis of HCC is the second-line non-invasive imaging (MRI, CT). These imaging modalities are known to have a diagnostic accuracy of 80% and 68%, respectively. However, we know that that these performances further decrease to 77% and 64%, respectively, when dealing with sub-centimetric HCC [5].

Other invasive alternatives have been proposed, namely a CT during hepatic arteriography (CTHA) or arterial portography (CTHP). These modalities, only applied in the subset of patients scheduled for treatment, had been investigated against Digital Subtraction Angiography (DSA) acquisition, demonstrating a clear superiority in terms of lesions identification (sensitivity CTHP 93.9%, CTHA 96.7%; CBCT pooled sensitivity 90% [95%VI 82%-95%]). [28-30].

More recently, CBCT has gained a role in assisting TACE procedures [12, 14], but all the existing reports in literature were focused on CBCT sensitivity (pooled sensitivity 90%[95%CI 82%-95%]); in case of diameter < 10 mm, sensitivity 94.5%) [30, 31]. Moreover, some Authors reported the ability of CBCT, generally in arterial phase only, to detect occult hepatic lesions (ranging: 11.5-28.7%) [15, 16]. However, the lack of delayed-phase imaging in the reported studies limited lesions' characterization (specificity). Therefore, the introduction of a biphasic approach in CBCT, including arterial and delayed phase, may combine the ability

to detect with the possibility to characterize HVF by applying the LI-RADS criteria[26] to DP-CBCT. Thus, by introducing in clinical practice the DP-CBCT imaging, and by applying the same SLIM radiological methodology to diagnose HVF, it could be possible to intra-procedurally characterize occult nodules. In order to strengthen this evidence, all the lesions in the present study were followed-up until a definitive radiological diagnosis was reached. By employing this approach, intraprocedural DP-CBCT detected 259 HVF, with 244 of them presenting a typical radiological wash-out and, therefore, appearing to address the features of an HCC. Thanks to these results, this approach led to a sensitivity, specificity, PPV and NPV of 99%, 89%, 99%, and 92%, respectively. Despite guidelines[1] did not consider reliable the radiological diagnosis of HVF with a diameter < 10 mm, intra-procedural DP-CBCT had sensitivity 100%, specificity 78%, PPV 95%, NPV 100% and accuracy 89% in this specific subset.

Comparing the intra- with the pre-procedural images, a datum emerged that 57 HCC were diagnosed only with DP-CBCT. More in detail, 54/57 (94.7%) lesions were confirmed by RS, reflecting the superiority in NPV of intra-procedural DP-CBCT over pre-procedural SLIM (92% vs overall SLIM 29.9%; vs MRI 30.8%; vs MDCT 29.7%). Only three of 57 (5.3%) lesions were not confirmed by RS (33/54 [61.1%] > 10 mm; 21/54 [38.9%] <10 mm). All the false positive HCC were HVF both in DP-CBCT and in RS, but without significant wash-out in RS. The diameter and the maximum follow-up time were 23, 9 and 8 mm, and 29, 28 and 28 days, respectively. These findings may reflect an incomplete maturation phase of the malignant process and could not be objectified due to unavailable follow-up. Since this approach to DP-CBCT imaging (using as diagnostic tool by applying LI-RADS criteria) was still under investigation the occult nodules observed were never treated during the same TACE procedure.

The stratification of occult nodules by diameter may have a clinical implication: occult HCC > 10 mm could represent a potential target for adjunctive treatment whereas occult HCC < 10 mm may identify impact on surveillance time frame. Further studies are necessary to better understand these implications.

According to Bland-Altman analysis, intra-procedural DP-CBCT systematically oversized the hyper-vascular HCC over the pre-procedural SLIM (mean diameter difference 1.6 mm or + 7.5%). This finding is consistent with previous reports [15], potentially reflecting the intrinsically higher signal-to-noise ratio of CBCT over MDCT, and the intra-arterial injection of contrast media.

Differences in HCC's detection rate and dimensions between pre-procedural SLIM and DP-CBCT may have a strong impact on the management of cirrhotic patients with HCC. In fact, both guidelines for HCC management [7, 32-34] and for liver transplantation [35] consider these two features as a cornerstone in the decision making process. Therefore, a more precise staging of the disease could facilitate a tailored treatment.

Our study presents some limitations. Firstly, the nature of the study is retrospective and observational. Secondly, the median time frame between pre-procedural SLIM and DP-CBCT was 46.0 days (95%CI 36.5-55.0), thus potentially justifying the differences of the lesion diameters observed in our results. However, we should underline that HCC is known to have a slow tumor volume doubling time (127.6 ± 128.7 days), typically longer respect to the time frame observed in our analysis [36]. Thirdly, being the design of this study retrospective and pragmatic (not a trial), it reflected the everyday clinical activity of a high-volume radiology department within a transplant center in which different SLIM are offered. Lastly, all dataset of images were reviewed in consensus and not in blinded fashion by three radiologist.

Conclusion

The present study highlights the better diagnostic performance of intra-procedural DP-CBCT over pre-procedural SLIM. This result presents relevant potential clinical implications in terms of treatment and surveillance timing.

Conflict of Interest and Authorship Conformation Form

Please check the following as appropriate:

- ✓ All authors have participated in (a) conception and design, or analysis and interpretation of the data; (b) drafting the article or revising it critically for important intellectual content; and (c) approval of the final version.
- ✓ This manuscript has not been submitted to, nor is under review at, another journal or other publishing venue.
- ✓ The authors have no affiliation with any organization with a direct or indirect financial interest in the subject matter discussed in the manuscript
- o The following authors have affiliations with organizations with direct or indirect financial interest in the subject matter discussed in the manuscript:

References

[1] L. European Association For The Study Of The, R. European Organisation For, C. Treatment Of, EASL-EORTC clinical practice guidelines: management of hepatocellular carcinoma, Journal of hepatology 56(4) (2012) 908-43.
[2] A. Forner, M. Reig, J. Bruix, Hepatocellular carcinoma, Lancet 391(10127) (2018) 1301-1314.
[3] e.e.e. European Association for the Study of the Liver. Electronic address, L. European Association for the Study of the, EASL Clinical Practice Guidelines: Management of hepatocellular carcinoma, Journal of hepatology 69(1) (2018) 182-236.
[4] R. Chou, C. Cuevas, R. Fu, B. Devine, N. Wasson, A. Ginsburg, B. Zakher, M. Pappas, E. Graham, S.D. Sullivan, Imaging Techniques for the Diagnosis of Hepatocellular Carcinoma: A Systematic Review and Meta-analysisImaging Techniques for Diagnosis and Staging of Hepatocellular Carcinoma, Annals of internal medicine 162(10) (2015) 697-711.
[5] Y.J. Lee, J.M. Lee, J.S. Lee, H.Y. Lee, B.H. Park, Y.H. Kim, J.K. Han, B.I. Choi, Hepatocellular Carcinoma: Diagnostic Performance of Multidetector CT and MR Imaging—A Systematic Review and Meta-Analysis, Radiology 275(1) (2015) 97-109.
[6] A.S. Kierans, S.K. Kang, A.B. Rosenkrantz, The Diagnostic Performance of Dynamic Contrast-enhanced MR Imaging for Detection of Small Hepatocellular Carcinoma Measuring Up to 2 cm: A Meta-Analysis, Radiology 278(1) (2016) 82-94.
[7] A. Forner, M.E. Reig, C. Rodriguez de Lope, J. Bruix, Current Strategy for Staging and Treatment: The BCLC Update and Future Prospects, Seminars in liver disease 30(01) (2010) 061-074.
[8] A. Basile, G. Carrafiello, A.M. Ierardi, D. Tsetis, E. Brountzos, Quality-improvement guidelines for hepatic transarterial chemoembolization, Cardiovascular and interventional radiology 35(4) (2012) 765-74.
[9] R.C. Gaba, R.P. Lokken, R.M. Hickey, A.J. Lipnik, R.J. Lewandowski, R. Salem, D.B. Brown, T.G. Walker, J.E. Silberzweig, M.O. Baerlocher, A.M. Echenique, M. Midia, J.W. Mitchell, S.A. Padia, S. Ganguli, T.J. Ward, J.L. Weinstein, B. Nikolic, S.R. Dariushnia, Quality Improvement Guidelines for Transarterial Chemoembolization and Embolization of Hepatic Malignancy, Journal of vascular and interventional radiology : JVIR 28(9) (2017) 1210-1223.e3.
[10] V. Tacher, A. Radaelli, M. Lin, J.-F. Geschwind, How I Do It: Cone-Beam CT during Transarterial Chemoembolization for Liver Cancer, Radiology 274(2) (2015) 320-334.
[11] P. Lucatelli, M. Corona, R. Argiro, M. Anzidei, G. Vallati, F. Fanelli, M. Bezzi, C. Catalano, Impact of 3D Rotational Angiography on Liver Embolization Procedures: Review of Technique and Applications, Cardiovascular and interventional radiology 38(3) (2015) 523-35.
[12] P. Lucatelli, R. Argiro, S. Bascetta, L. Saba, C. Catalano, M. Bezzi, G.B. Levi Sandri, Single injection dual phase CBCT technique ameliorates results of trans-arterial chemoembolization for hepatocellular cancer, Translational gastroenterology and hepatology 2 (2017) 83.
[13] R. Loffroy, M. Lin, G. Yenokyan, P.P. Rao, N. Bhagat, N. Noordhoek, A. Radaelli, J. Blijd, E. Liapi, J.F. Geschwind, Intraprocedural C-arm dual-phase cone-beam CT: can it be used to predict short-term response to TACE with drug-eluting beads in patients with hepatocellular carcinoma?, Radiology 266(2) (2013) 636-48.
[14] B. Bapst, M. Lagadec, R. Breguet, V. Vilgrain, M. Ronot, Cone Beam Computed Tomography (CBCT) in the Field of Interventional Oncology of the Liver, Cardiovascular and interventional radiology 39(1) (2016) 8-20.
[15] P. Lucatelli, R. Argiro, S. Ginanni Corradini, L. Saba, C. Cirelli, F. Fanelli, C. Ricci, G.B. Levi Sandri, C. Catalano, M. Bezzi, Comparison of Image Quality and Diagnostic Performance of Cone-Beam CT during Drug-Eluting Embolic Transarterial Chemoembolization and Multidetector CT in the Detection of Hepatocellular Carcinoma, Journal of vascular and interventional radiology : JVIR 28(7) (2017) 978-986.
[16] M. Jonczyk, J. Chapiro, F. Collettini, D. Geisel, D. Schnapauff, F. Streitparth, T. Schmidt, B. Hamm, B. Gebauer, G. Wieners, Diagnostic Accuracy of Split-Bolus Single-Phase Contrast-Enhanced Cone-Beam CT for the Detection of Liver Tumors before Transarterial Chemoembolization, Journal of vascular and interventional radiology : JVIR 28(10) (2017) 1378-1385.
[17] L. Lechuga, G.A. Weidlich, Cone Beam CT vs. Fan Beam CT: A Comparison of Image Quality and Dose Delivered Between Two Differing CT Imaging Modalities, Cureus 8(9) (2016) e778-e778.

[18] A.C. Larson, T.K. Rhee, J. Deng, D. Wang, K.T. Sato, R. Salem, T. Paunesku, G. Woloschak, M.F. Mulcahy, D. Li, R.A. Omary, Comparison between intravenous and intraarterial contrast injections for dynamic 3D MRI of liver tumors in the VX2 rabbit model, Journal of Magnetic Resonance Imaging 24(1) (2006) 242-247.
[19] J.F. Cohen, D.A. Korevaar, D.G. Altman, D.E. Bruns, C.A. Gatsonis, L. Hooft, L. Irwig, D. Levine, J.B. Reitsma, H.C.W. de Vet, P.M.M. Bossuyt, STARD 2015 guidelines for reporting diagnostic accuracy studies: explanation and elaboration, BMJ Open 6(11) (2016) e012799.
[20] M.D. Martino, M. Rossi, G. Mennini, F. Melandro, M. Anzidei, S.D. Vizio, K. Koryukova, C. Catalano, Imaging follow-up after liver transplantation, The British journal of radiology 89(1064) (2016) 20151025.
[21] M. Ciolina, M. Di Martino, O. Bruno, R. Pommier, V. Vilgrain, M. Ronot, Peritoneal and pleural fluids may appear hyperintense on hepatobiliary phase using hepatobiliary MR contrast agents, European Radiology 28(7) (2018) 3020-3031.
[22] F.E. Boas, B. Do, J.D. Louie, N. Kothary, G.L. Hwang, W.T. Kuo, D.M. Hovsepian, M. Kantrowitz, D.Y. Sze, Optimal imaging surveillance schedules after liver-directed therapy for hepatocellular carcinoma, Journal of vascular and interventional radiology : JVIR 26(1) (2015) 69-73.
[23] J.Y. Choi, J.M. Lee, C.B. Sirlin, CT and MR imaging diagnosis and staging of hepatocellular carcinoma: part I. Development, growth, and spread: key pathologic and imaging aspects, Radiology 272(3) (2014) 635-54.
[24] J. Bruix, M. Sherman, D. American Association for the Study of Liver, Management of hepatocellular carcinoma: an update, Hepatology 53(3) (2011) 1020-2.
[25] J.A. Marrero, L.M. Kulik, C.B. Sirlin, A.X. Zhu, R.S. Finn, M.M. Abecassis, L.R. Roberts, J.K. Heimbach, Diagnosis, Staging, and Management of Hepatocellular Carcinoma: 2018 Practice Guidance by the American Association for the Study of Liver Diseases, Hepatology 68(2) (2018) 723-750.
[26] V. Chernyak, K.J. Fowler, A. Kamaya, A.Z. Kielar, K.M. Elsayes, M.R. Bashir, Y. Kono, R.K. Do, D.G. Mitchell, A.G. Singal, A. Tang, C.B. Sirlin, Liver Imaging Reporting and Data System (LI-RADS) Version 2018: Imaging of Hepatocellular Carcinoma in At-Risk Patients, Radiology 289(3) (2018) 816-830.
[27] H.-C. Kim, Role of C-Arm Cone-Beam CT in Chemoembolization for Hepatocellular Carcinoma, Korean J Radiol 16(1) (2015) 114-124.
[28] S. Miyayama, M. Yamashiro, M. Okuda, Y. Yoshie, N. Sugimori, S. Igarashi, Y. Nakashima, O. Matsui, Usefulness of cone-beam computed tomography during ultraselective transcatheter arterial chemoembolization for small hepatocellular carcinomas that cannot be demonstrated on angiography, Cardiovascular and interventional radiology 32(2) (2009) 255-64.
[29] S. Miyayama, M. Yamashiro, Y. Hattori, N. Orito, K. Matsui, K. Tsuji, M. Yoshida, O. Matsui, Efficacy of cone-beam computed tomography during transcatheter arterial chemoembolization for hepatocellular carcinoma, Japanese journal of radiology 29(6) (2011) 371-7.
[30] L. Pung, M. Ahmad, K. Mueller, J. Rosenberg, C. Stave, G.L. Hwang, R. Shah, N. Kothary, The Role of Cone-Beam CT in Transcatheter Arterial Chemoembolization for Hepatocellular Carcinoma: A Systematic Review and Meta-analysis, Journal of vascular and interventional radiology : JVIR 28(3) (2017) 334-341.
[31] X. Wang, H. Yarmohammadi, G. Cao, X. Ji, J. Hu, H. Yarmohammadi, H. Chen, X. Zhu, R. Yang, S. Solomon, Dual phase cone-beam computed tomography in detecting <3 cm hepatocellular carcinomas during transarterial chemoembolization, Journal of Cancer Research and Therapeutics 13(1) (2017) 38-43.
[32] A. Vogel, A. Cervantes, I. Chau, B. Daniele, J. Llovet, T. Meyer, J.C. Nault, U. Neumann, J. Ricke, B. Sangro, P. Schirmacher, C. Verslype, C.J. Zech, D. Arnold, E. Martinelli, E.G. Committee, Hepatocellular carcinoma: ESMO Clinical Practice Guidelines for diagnosis, treatment and follow-up, Annals of oncology : official journal of the European Society for Medical Oncology 29(Supplement_4) (2018) iv238-iv255.
[33] P.R. Galle, A. Forner, J.M. Llovet, V. Mazzaferro, F. Piscaglia, J.-L. Raoul, P. Schirmacher, V. Vilgrain, EASL Clinical Practice Guidelines: Management of hepatocellular carcinoma, Journal of hepatology 69(1) (2018) 182-236.
[34] EASL-EORTC clinical practice guidelines: management of hepatocellular carcinoma, Journal of hepatology 56(4) (2012) 908-43.
[35] V. Mazzaferro, E. Regalia, R. Doci, S. Andreola, A. Pulvirenti, F. Bozzetti, F. Montalto, M. Ammatuna, A. Morabito, L. Gennari, Liver transplantation for the treatment of small hepatocellular carcinomas in patients with cirrhosis, The New England journal of medicine 334(11) (1996) 693-9.

[36] C. An, Y.A. Choi, D. Choi, Y.H. Paik, S.H. Ahn, M.-J. Kim, S.W. Paik, K.-H. Han, M.-S. Park, Growth rate of early-stage hepatocellular carcinoma in patients with chronic liver disease, Clin Mol Hepatol 21(3) (2015) 279-286.

Figure and Table Captions

Figure 1. Flowchart 1.

Figure1. Detailed Flowchart of the study. The number of nodules was calculated based on follow-up SLIM

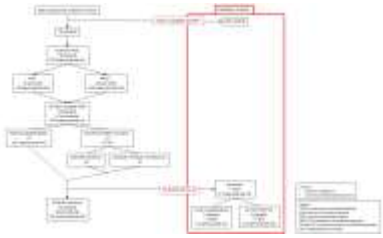

Figure 2. Time Frame

Figure 2 showed the time between pre-procedural second line imaging modality (SLIM) and trans-arterial chemoembolization (TACE) among all patients (first column) and the required minimum time for the definitive radiological diagnosis only in patients with occult HCCs (second columns)

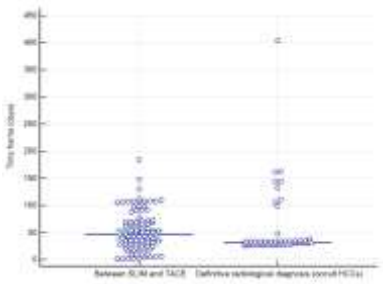

Figure 3. Flowchart 2.

Figure 3 showed the flowchart of occult hyper-vascular foci distribution. HCC hepatocellular carcinoma; DM diameter maximum

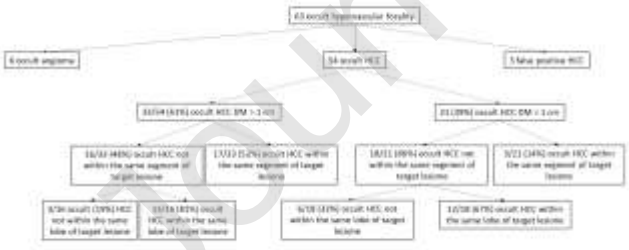

Figure 4. Clinical Case

Figure 4 Clinical case of 54 years old woman with single HCC in V-VIII hepatic segment (arrow) showed at magnetic resonance imaging in arterial (a) and hepatobiliary phase (b), without any other nodules; the cone beam computed tomography performed during TACE after 31 days evidenced the target nodule (arrow) and another hyper-vascular focality (arrowhead) in the II hepatic segment with wash-in (c) and wash-out in

the delayed phase (d) suspected for occult HCC. The follow-up CT confirmed the findings with typical rapid wash-in (e) and wash-out (f) (arrowhead) consisted with HCC. The arrow in figure e and f highlighted the complete response dot the target nodules

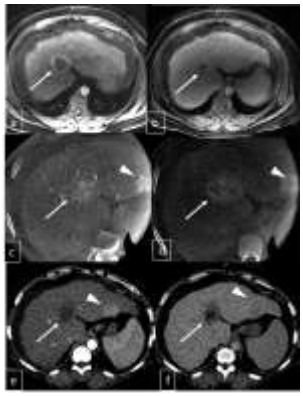

Figure 5. ROC Curve Comparison

Figure 5 ROC curve analysis. HCC hepatocellular carcinoma; CBCT cone beam computed tomography; SLIM second line imaging modality; DM diameter maximum; MRI magnetic resonance imaging; MDCT multidetector computed tomography

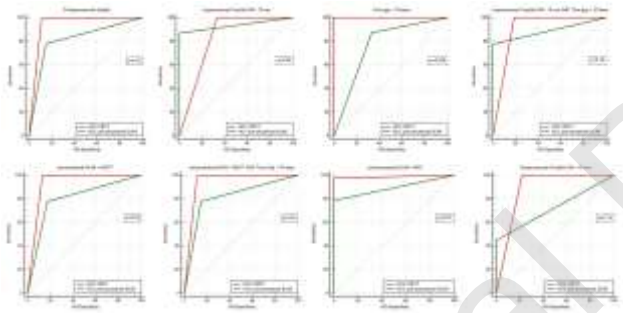

Figure 6. Bland and Altman plot

Figure 6 The Bland and Altman plot showed mean diameter differences between intra-procedural CBCT and pre-procedural SLIM). DM: diameter maximum; CBCT: come beam CT; SLIM: second line imaging modality.

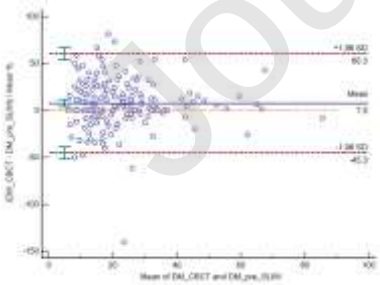

Table 1. Clinical demographic

TACE Trans arterial chemoembolization; SD Standard Deviation; M Male; F Female; HCV Hepatitis C virus; HBV Hepatitis B virus; NASH Non-alcoholic steatohepatitis; MELD Model for End-Stage Liver Disease;

Patient number	N= 72
Number of TACE performed	N= 90
Nodules Dimension **Maximum diameter. mm. (mean value 95%CI. range)**	 16.0 mm (15.0-19.7; 6.0-89.0)
Age, year (mean value ± SD. range)	66.5± 12.8 (41-89)
Sex (M/F)	50/22
Child Pugh N (%) **A5** **A6** **B7** **B8** **B9**	 34 (47.2) 12 (16.7) 18 (25) 7 (9.7) 1 (1.4)
BCLC N (%) **A** **B**	 46 (63.9) 26 (36.1)
Etiology: N (%) **HCV** **HBV** **Alcohol related cirrhosis** **Cryptogenetic cirrhosis** **NASH**	 29 (40.3) 19 (26.4) 15 (20.8) 5 (6.9) 4 (5.6)
MELD: N (%) **<10** **≥10**	 42 (58.3) 30 (41.7)
MELDNa: N (%) **<10** **≥10**	 48 (66.7) 24 (33.3)
Mono-focal N (%) / multi-focal disease N (%)	22 (30.6)/ 50 (69.4)
Indications for TACE N (%) **Palliative** **Bridging** **Debulking** **Downstaging**	 48 (53.3) 25 (27.8) 8 (8.9) 9 (10.0)

Table 2. Diagnostic performance

RS: reference standard; CI 95%: Confidence interval 95%; SLIM second line imaging modality; HVF hyper-vascular foci; MRI: magnetic resonance imaging; MDCT: multidetector computed tomography; The diagnostic performance of MRI pre-procedural < 30 days was not determined due to few data available.

Diagnostic exams vs RS	Sensitivity (%) [CI95%]	Specificity (%) [CI95%]	Positive predictive value (%) [CI95%]	Negative predictive value (%) [CI95%]	Accuracy (%) [CI95%]
SLIM pre-procedural	77.78 [72.0 - 82.8]	85.19 [66.3 - 95.8]	97.9 [95.0 - 99.2]	29.9 [24.3 - 36.1]	81.5 [76.3 – 85.9]
SLIM pre-procedural HVF >10 mm	86.91 [81.3 - 91.3]	100.00 [29.2 - 100.0]	100.0 [100 - 100]	10.7 [7.7 - 14.7]	93.5 [89.0 -96.5]
SLIM pre-procedural <30 days	87.32 [77.3 - 94.0]	66.67 [22.3 - 95.7]	96.9 [90.9 - 99.0]	30.8 [16.2 - 50.5]	77.0 [66.0 – 85.8]
SLIM pre-procedural HVF >10 mm <30 days	77.50 [71.7 - 82.6]	100.00 [79.4 - 100.0]	100.0 [100 - 100]	22.9 [19.0 - 27.3]	88.8 [84.2 – 92.3]
MRI pre-procedural	78.57 [63.2 - 89.7]	100.00 [39.8 - 100.0]	100.0 [100 - 100]	30.8 [19.9 - 44.2]	89.3 [76.6 – 96.5]
MDCT pre-procedural	77.61 [71.2 - 83.2]	82.61 [61.2 - 95.0]	97.5 [94.1 - 99.0]	29.7 [23.5 - 36.7]	80.1 [74.3 - 0.851]
CBCT	99.18 [97.1 - 99.9]	88.89 [70.8 - 97.6]	98.8 [96.5 - 99.6]	92.3 [75.0 - 98.0]	94.0 [90.5 – 96.5]
CBCT HVF >10 mm	100.00 [98.1 - 100.0]	66.67 [9.4 - 99.2]	99.5 [97.5 - 99.9]	100.0 [100 - 100]	83.3 [77.3 – 88.3]
CBCT HVF <10 mm	100.00 [90.7 - 100.0]	77.78 [40.0 - 92.7]	95.0 [84.8 – 98.5]	100.0 [100 - 100]	88.9 [76.3-96.2]